Mechanism of Aminoglycoside Antibiotic Kinase APH(3′)-IIIa: Role of the Nucleotide Positioning Loop†

Paul R. Thompson,‡ David D. Boehr,‡ Albert M. Berghuis,§ and Gerard D. Wright*

Department of Biochemistry, Antimicrobial Research Centre, McMaster University, Hamilton, Ontario, Canada L8N 3Z5

Received February 12, 2002; Revised Manuscript Received April 5, 2002

ABSTRACT: The aminoglycoside antibiotic resistance kinases (APHs) and the Ser/Thr/Tyr protein kinases share structural and functional homology but very little primary sequence conservation (<5%). A region of structural, but not amino acid sequence, homology is the nucleotide positioning loop (NPL) that closes down on the enzyme active site upon binding of ATP. This loop region has been implicated in facilitating phosphoryl transfer in protein kinases; however, there is no primary sequence conservation between APHs and protein kinases in the NPL. There is an invariant Ser residue in all APH NPL regions, however. This residue in APH(3′)-IIIa (Ser27), an enzyme widespread in aminoglycoside-resistant Enterococci, Streptococci, and Staphylococci, directly interacts with the β-phosphate of ATP through the Ser hydroxymethyl group and the amide hydrogen in the 3D structure of the enzyme. Mutagenesis of this residue to Ala and Pro supported a role for the Ser amide hydrogen in nucleotide capture and phosphoryl transfer. A molecular model of the proposed dissociative transition state, which is consistent with all of the available mechanistic data, suggested a role for the amide of the adjacent Met26 in phosphoryl transfer. Mutagenesis studies confirmed the importance of the amide hydrogen and suggest a mechanism where Ser27 anchors the ATP β-phosphate facilitating bond breakage with the γ-phosphate during formation of the metaphosphate-like transition, which is stabilized by interaction with the amide hydrogen of Met26. The APH NPL therefore acts as a lever, promoting phosphoryl transfer to the aminoglycoside substrate, with the biological outcome of clinically relevant antibiotic resistance.

A common mechanism of bacterial resistance to the clinically important aminoglycoside antibiotics is through chemical modification by phosphoryl transfer from ATP, a reaction catalyzed by a family of kinases termed aminoglycoside phosphotransferases (APHs).[1] The APHs are structurally homologous to eukaryotic Ser/Thr and Tyr protein kinases (*1*), despite very low amino acid sequence similarity (<5%). These enzymes consist of two domains, an N-terminal β-strand-rich domain and a C-terminal α-helical domain, separated by the active site cleft. APHs are also functionally similar to protein kinases with the ability to bind and phosphorylate peptide substrates on Ser residues (*2*).

In principle, a thorough understanding of enzyme mechanism, including transition state structure, could be exploited in the generation of specific potent inhibitors of APHs that could find clinical utility in reversing antibiotic resistance. The determination of the three-dimensional structure of the enzyme APH(3′)-IIIa (*1*), which is responsible for resistance to a broad spectrum of aminoglycoside antibiotics in Gram-positive pathogens such as the Enterococci, Staphylococci, and Streptococci, has facilitated investigation on the mechanism of phosphoryl transfer by this class of resistance enzyme. There are five absolutely conserved residues among APHs and protein kinases that line the catalytic core (*1*). One of these residues, Asp190, which is equivalent to the invariant Asp of protein kinases that has been suggested to be an active site base (e.g., Asp166 in protein kinase A), does not act as a classical general base in APH(3′)-IIIa, but results do suggest that this residue is important for aminoglycoside and metal ion positioning for productive phosphoryl transfer (*3*). Another conserved residue, Asp208 (equivalent to Asp184 in protein kinase A), which coordinates both Mg^{2+} ions in the active site, is critical for catalysis as mutation to Ala, Asn, or Glu abolishes kinase activity; these results and others have demonstrated that Asp208 is important to transition state (TS) stabilization (*3*). Taken together, these studies have demonstrated that initial deprotonation of the aminoglycoside hydroxyl group to be phosphorylated is not essential for phosphate transfer. Phosphoryl transfer therefore likely proceeds through a dissociative-like mechanism with substantial P−O−P bond breakage prior to transfer to the incoming hydroxyl, generating an electrophilic metaphosphate-like TS.

In addition to these conserved active site residues, protein and aminoglycoside kinases also share a Gly-rich loop that plays a role in ATP binding. This loop is located in the N-terminal domain between the first and second β-strands of the antiparallel β-sheet (Figure 1A) (*1*). In protein kinases,

† This work was supported by Grants MT-13536 (G.D.W.) and MOP-13107 (A.M.B.) from the Canadian Institutes of Health Research.

* To whom correspondence should be addressed. Phone: 905-525-9140 ext 22454. Fax: 905-522-9033. E-mail: wrightge@mcmaster.ca.

‡ These authors contributed equally to this work.

§ Present address: Departments of Biochemistry and Microbiology & Immunology, McGill University, Lyman Duff Medical Sciences Building, 3775 University St., Montreal, Québec, Canada H3A 2B4.

[1] Abbreviations: APH, aminoglycoside antibiotic phosphotransferase; NPL, nucleotide positioning loop; TS, transition state; MIC, minimal inhibitory concentration.

10.1021/bi0256680 CCC: $22.00
Published on Web 05/09/2002

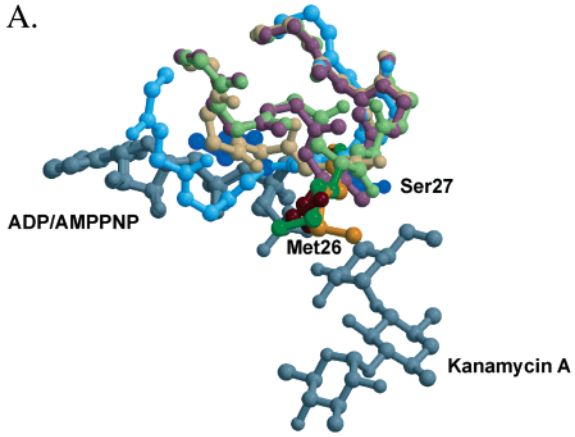

B.

APH(3')-VIIa	12	-	-	K	C	S	-	-	-	E	G	M	S	P	A	E	V	Y	K	C
APH(3')-Vc	11	H	Y	E	W	T	S	V	N	E	G	D	S	G	A	S	V	Y	R	L
APH(3')-IIa	22	-	Y	D	W	A	Q	Q	T	I	G	C	S	D	A	A	V	F	R	L
APH(3')-Ic	26	-	Y	R	W	A	R	D	N	V	G	Q	S	G	A	T	I	Y	R	L
APH(3')-IIIa	**16**	**K**	**Y**	**R**	**C**	**V**	**K**	**D**	**T**	**E**	**G**	**M**	**S**	**P**	**A**	**K**	**V**	**Y**	**K**	**L**
							*	*	*	*	*	*	*	*						

FIGURE 1: NPL region of APH(3′). (A) Overlap of NPL regions from APH(3′)-IIIa crystal structures. The structures of ADP, AMPPNP, and kanamycin are in gray; the NPL in the unliganded form of the enzyme is in blue while the AMPPNP-bound form is in green; the ADP−kanamycin A bound form is in yellow; and the ADP-bound form is in red. Only the Met26 and Ser27 side chains are shown. (B) Sequence comparisons of the APH(3′) family of enzymes. Asterisks indicate the NPL region. Only Gly25 and Ser27 are absolutely conserved.

the Gly-rich or nucleotide positioning loop (NPL) has the consensus sequence GXGXXG, and mutagenesis of these Gly residues to Ser or Ala is detrimental to enzymatic activity (*4*−*6*). It has been postulated that the flexibility of the loop may be required for controlling the relative affinities for ATP and ADP (*6*) and the loop may also be involved in the phosphoryl transfer step itself (*5*). Ser53, at the apex of the NPL in protein kinase A, has been suggested to interact with the γ-phosphate to aid in phosphoryl transfer (*7*). The backbone amide of Ser53 forms a hydrogen bond with an axial oxygen of the γ-phosphate and, on the basis of the results for the Ser53Pro mutation, appears to be required for efficient catalysis, although the side chain hydroxymethyl group is not (*7*).

The NPL in APH(3′)-IIIa, like its protein kinase counterparts, is highly mobile, and its conformation is sensitive to the ligands occupying the active site (*8*). However, in APH(3′)-IIIa the NPL is distinct from its protein kinase counterpart in important ways. First, it does not share the GXGXXG consensus sequence, and second, the loop is one residue longer than its protein kinase counterparts, resulting in a wider turn. The APH(3′) family of enzymes contains an absolutely conserved Ser [Ser27 in APH(3′)-IIIa] in the NPL. The side chain hydroxyl of this residue forms a hydrogen bond to a nonbridge oxygen on the β-phosphate in structures of APH(3′)-IIIa with bound ADP (*1*) and with AMPPNP (*8*). However, in the presence of aminoglycoside and ADP, there is a conformational change in the NPL such that the Ser main chain rotates, resulting in the formation of an additional hydrogen bond to this β-phosphate by the backbone amide (*9*).

With these differences and similarities in protein kinase and APH NPLs in mind, we wished to determine the contribution of the NPL to rate enhancement in APH(3′)-IIIa. Molecular modeling has enabled us to predict a unique hydrogen bond donation from the backbone amide of Met26 in the NPL to the γ-phosphate during catalysis that is not apparent in any of the ground state structures. The addition of a hydrogen bond donor by the Ser27 backbone amide may play a part in the positioning of this residue for this interaction, although comparisons of site mutants suggest that Ser27 also plays another role(s). We propose a mechanism whereby the NPL helps to promote the formation of a metaphosphate-like TS required for phosphoryl transfer, resulting in antibiotic inactivation.

EXPERIMENTAL PROCEDURES

Chemicals. Ribostamycin, lividomycin, neomycin B, butirosin, amikacin, β-NADH, phosphoenolpyruvate, and PK/LDH enzymes were from Sigma (St. Louis, MO). ATPγS was from Boehringer-Mannheim, and kanamycin A was from Bioshop (Burlington, Ontario, Canada). Oligonucleotide primers were purchased from the Central Facility of the Institute for Molecular Biology and Biotechnology, McMaster University.

Site-Directed Mutagenesis and Protein Purification. The generation of Ser27Ala/Pro and Met26Ala/Pro mutants was undertaken according to the QuikChange method (Stratagene, LaJolla, CA), using single sets of degenerate mutagenesis primers. Positive clones were sequenced in their entirety at the Central Facility of the Institute for Molecular Biology and Biotechnology, McMaster University. The purification of APH(3′)-IIIa has been described previously (*10*), and the mutant enzymes were purified in an analogous manner.

Enzyme Assay. APH(3′)-IIIa was assayed by coupling ADP release to the activity of pyruvate kinase and lactate dehydrogenase as previously described (*10*). Initial rates were

Table 1: Steady-State Kinetic Parameters for Mutant APH(3′)-IIIa Proteins[a]

substrate	K_M (μM)	k_{cat} (s^{-1})	k_{cat}/K_M ($M^{-1}\,s^{-1}$)	$k_{cat(WT)}/k_{cat(mut)}$	$(k_{cat}/K_M)_{WT}/(k_{cat}/K_M)_{mut}$
		Wild Type			
ATP	27.7 ± 3.7	1.76 ± 0.08	6.4×10^4		
kanamycin A	12.6 ± 2.6	1.79 ± 0.09	1.4×10^5		
neomycin B	7.72 ± 0.9	2.08 ± 0.07	2.7×10^5		
amikacin	245 ± 27	2.46 ± 0.11	1.0×10^4		
butirosin	34.3 ± 3.1	2.02 ± 0.07	5.9×10^4		
ribostamycin	9.3 ± 1.8	1.89 ± 0.10	2.0×10^5		
		APH(3′)-IIIa Ser27Ala			
ATP	54.4 ± 6.5	0.51 ± 0.02	9.4×10^3	3.5	6.8
kanamycin A	15.0 ± 3.7	0.61 ± 0.03	4.1×10^4	2.9	3.5
neomycin B[b]		0.28 ± 0.02		7.4	
amikacin	574 ± 162	0.32 ± 0.04	5.6×10^2	7.7	18
ribostamycin	13.9 ± 3.8	0.68 ± 0.03	4.9×10^4	2.8	4.1
		APH(3′)-IIIa Ser27Pro			
ATP[c]	32.3 ± 3.9	0.056 ± 0.001	1.7×10^3	31	37
kanamycin A	11.9 ± 1.7	0.038 ± 0.001	3.2×10^3	47	45
neomycin B[d]		0.0518 ± 0.0004		40	
amikacin[e]		≤0.009 ± 0.0004		273	
butirosin	122.3 ± 33.4	0.021 ± 0.002	1.7×10^2	96	346
ribostamycin	5.0 ± 0.7	0.047 ± 0.001	9.4×10^3	40	22
		APH(3′)-IIIa Met26Ala			
ATP	4.89 ± 0.43	0.69 ± 0.01	1.4×10^5	2.6	0.45
kanamycin A	22.4 ± 3.5	0.72 ± 0.01	3.2×10^4	2.5	4.4
neomycin B	7.91 ± 1.09	0.83 ± 0.02	1.1×10^5	2.5	2.4
amikacin	274 ± 18	0.70 ± 0.02	2.5×10^3	3.5	4
butirosin	12.9 ± 2.0	0.89 ± 0.03	6.9×10^4	2.3	0.85
ribostamycin	9.63 ± 1.01	0.69 ± 0.02	7.2×10^4	2.7	2.8
		APH(3′)-IIIa Met26Pro			
ATP	28.1 ± 4.4	0.12 ± 0.01	4.4×10^3	15	14
kanamycin A	15.7 ± 2.8	0.15 ± 0.01	9.8×10^3	12	14
neomycin B	9.76 ± 2.22	0.21 ± 0.01	2.2×10^4	10	12
amikacin	424 ± 46	0.07 ± 0.00	1.8×10^2	35	56
butirosin	73.1 ± 7.8	0.20 ± 0.01	2.7×10^3	10	22
ribostamycin	13.4 ± 1.3	0.16 ± 0.01	1.2×10^4	12	17

[a] The values for wild-type (WT) parameters were taken from ref *10*. [b] The K_M for neomycin B could not be reliably determined, but we can estimate an upper limit of 3.5 μM. [c] Neomycin B was fixed at 100 μM. [d] V_{max} occurred at the lowest substrate concentration tested. The k_{cat} reported is an estimation using the data corresponding to 100 μM neomycin B and 1 mM ATP. [e] Amikacin was an exceptionally poor substrate for the Ser27Pro mutant. Thus an estimation of the k_{cat} was made using the rate of reaction observed at 1.5 mM amikacin and 1 mM ATP.

fit using the nonlinear least-squares method contained with the Grafit 4.0 software package (*11*) to either eq 1 or eq 2 if substrate inhibition was detected.

$$v = (k_{cat}/E_t)[S]/(K_M + [S]) \quad (1)$$

$$v = (k_{cat}/E_t)[S]/[(K_M + [S])(1 + [S]/K_i)] \quad (2)$$

The Mg^{2+} ion dependence of the mutant enzymes was determined as previously described (*3*).

Solvent viscosity effects and solvent isotope effects [H_2O content ≤3.5% (v/v)] were determined essentially as described (*12*). Glycerol was used as the microviscogen at concentrations from 0 to 30% (w/v), and the relative viscosity of the solutions was determined in quadruplicate using an Ostwald viscometer (*12*). Steady-state kinetic parameters were determined using the coupled assay described above.

Determination of Minimum Inhibitory Concentrations. The minimum inhibitory concentrations (MICs) for the mutants were determined according to the methods described in ref *3*, except for the replacement of sterile polypropylene microtiter plates for the polystyrene plates previously used. Polystyrene plates may bind positively charged compounds, such as aminoglycosides, and can cause a slight increase in the absolute values of MIC.

RESULTS

Kinetic Analyses of APH(3′)-IIIa Ser27Ala/Pro Mutants. Ser27 is absolutely conserved among APH(3′)'s (Figure 1B). The mutagenesis of Ser27 had a dramatic effect on the kinetic parameters for both ATP and a number of aminoglycoside substrates (Table 1). Both turnover rate (k_{cat}) and substrate capture (k_{cat}/K_M) (*13*) were significantly depressed in the mutants, where the decrease in k_{cat} was most responsible for the change in k_{cat}/K_M. The Ser27Pro mutation had the greatest effect, where it generally showed greater than a 10-fold further reduction in kinetic parameters compared to the Ser27Ala mutation (Table 1). These results are not due to misfolded enzymes, as protease sensitivity assays that detect unfolded regions of the protein are consistent with WT results (data not shown). Mutation of Ser27Pro (or Met26Pro; see below) has the potential to significantly disrupt local protein structure, either as a result of steric clashes due to the side chain or that appropriate Ψ and α angles are unattainable for a Pro residue in this position. Close inspection of the structure in the NPL indicates that the Pro mutations will not cause significant perturbations in the protein structure. Furthermore, experimental protease sensitivity assays that detect unfolded regions of the protein are consistent with WT results (data not shown). In our extensive experience

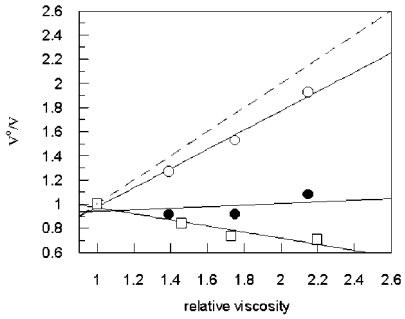

FIGURE 2: Solvent viscosity effect (SVE) on the steady-state kinetics of ATP utilization of APH(3′)-IIIa mutant proteins: Ser27Ala (□), Met26Ala (○), and Met26Pro (●). The SVE for WT enzyme approaches the theoretical maximum effect of 1 (dashed line), indicative of a viscosity-dependent rate-limiting step.

Table 2: Solvent Isotope Effects for APH(3′)-IIIa Wild-Type and Mutant Proteins

	$^{H}V/^{D}V$		$^{H}(V/K)/^{D}(V/K)$	
enzyme	ATP	kanamycin A	ATP	kanamycin A
WT	1.79 ± 0.02	1.67 ± 0.03	1.18 ± 0.09	0.98 ± 0.07
Ser27Ala	0.93 ± 0.04	0.90 ± 0.04	0.73 ± 0.11	0.98 ± 0.14
Met26Pro	1.24 ± 0.08	0.883 ± 0.079	1.21 ± 0.27	1.19 ± 0.34

with APH(3′)-IIIa, this is a highly sensitive assay of structural integrity.

The decrease in k_{cat} suggested that for the Ser27Ala mutant ADP release is no longer fully rate-limiting, which is the case for the wild-type enzyme (*12*, *14*). Solvent viscosity effects on ATP-dependent steady-state kinetics for this mutant (Figure 2, $SVE_V = -0.25 \pm 0.06$) are consistent with a viscosity-independent rate-limiting step, most likely the chemical step. The macroviscogen PEG 8000 [2.5% (w/v)] did not have a significant effect on APH(3′)-IIIa Ser27Ala activity or any of the other mutants tested (data not shown).

As with the WT and other mutants of APH(3′)-IIIa (*3*, *12*), the solvent isotope effects in D_2O for either ATP or kanamycin are not significant (Table 2), suggesting that deprotonation of the substrate alcohol is not important for rate enhancement in this mutant.

On the basis of our earlier work on the Mg^{2+} dependence of wild-type and mutant APH(3′)-IIIa proteins, which indicated the importance of metal ions to catalysis, we have examined the metal ion dependence of the Ser27Ala and the Ser27Pro mutants (Figure 3). In contrast to the WT enzyme, the Ser27 mutants do not demonstrate a dramatic decrease in rate with increasing Mg^{2+} concentrations.

Transition State Modeling. On the basis of the crystal structures of APH(3′)-IIIa in complex with the nonhydrolyzable ATP analogue AMPPNP (*8*) and in complex with ADP and the aminoglycoside antibiotic kanamycin A (*9*), models were constructed of the enzyme in complex with ATP and kanamycin and of the enzyme in complex with ADP and phosphorylated kanamycin. Construction of these models was trivial in that the differences observed in the active site between the different crystal structures are insignificant except for the NPL region. For the construction of the models the conformation of the NPL chosen was that from the crystal structure of APH(3′)-IIIa in complex with ADP and kanamycin, since other conformations were incompatible with a bound aminoglycoside. To construct a model of the transition state, a metaphosphate was placed in the crystal structure of

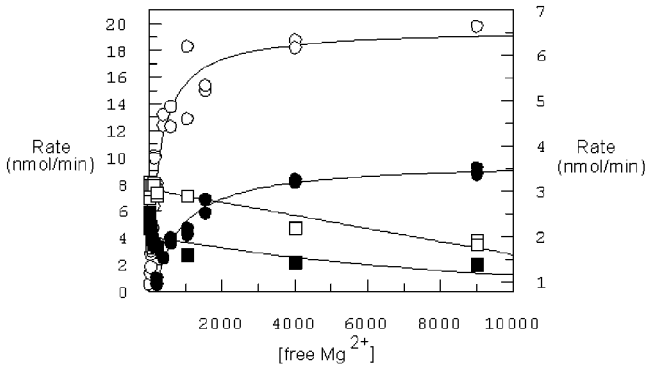

FIGURE 3: Magnesium ion dependence of Ser27 and Met26 mutant proteins. The initial rates obtained for Ser27Ala (○) and Met26Ala (■) were plotted using the left *Y*-axis whereas the initial rates obtained for the Ser27Pro (●) and Met26Pro (□) were plotted using the right *Y*-axis. The concentrations of ATP (1 mM) and kanamycin (100 μM) were fixed at 1 and 0.1 mM, respectively.

APH(3′)-IIIa + ADP + kanamycin A, exactly halfway between the positions of the ATP γ-phosphate and the kanamycin A phosphoryl group, obtained from the previous two models (Figure 4). This model is in agreement with a dissociative-like mechanism due to the distance between the metaphosphate and ADP and kanamycin (2.1−2.2 Å), which precludes the simultaneous existence of bonds between ADP, metaphosphate, and aminoglycoside. Intriguingly, the constructed models also predict the presence of a hydrogen bond between the Met26 backbone amide and one of the oxygens of the γ-phosphate/metaphosphate which is not observed in any of the crystal structures (Figure 4).

Kinetic Analyses of APH(3′)-IIIa Met26Ala/Pro Mutants. Structural modeling of APH(3′)-IIIa-catalyzed phosphoryl transfer indicated that a hydrogen bond between the backbone amide of Met26 to a metaphosphate-like intermediate or TS could occur. Consequently, we generated the Met26Ala and Met26Pro mutant proteins for in vitro and in vivo analyses to test this hypothesis. Met26 is not conserved among the APH(3′) family of enzymes (Figure 1B), and it was therefore not unexpected that mutation of this residue to Ala had little effect on enzyme activity (Table 1; only a modest decrease in k_{cat} of 2.3−3.5-fold). The wild-type enzyme follows a Theorell−Chance kinetic mechanism where K_M for ATP closely approximates K_d for this substrate and where ADP release is fully rate determining (*12*, *14*). Upon mutation of Met26 to Ala, the K_M for ATP decreases significantly (5.7-fold, Table 1), and the affinity for ADP may likewise decrease, resulting in a lowered rate for ADP release and a decreased k_{cat}. Indeed, comparable to the WT enzyme, k_{cat} for this mutant is largely viscosity dependent (Figure 2, $SVE_V = 0.80 \pm 0.05$), indicating that there is not a significant change to the contributions to product release that govern k_{cat}.

On the other hand, the Met26Pro mutant is significantly impaired in its ability to phosphorylate aminoglycosides (Table 1), where the majority of the effect is associated with a decrease in k_{cat} (10−35-fold). Unlike the Met26Ala mutant, the activity of Met26Pro is not affected by increases in viscosity (Figure 2) and likely suggests that, analogous to the Ser27 mutations, the phosphoryl transfer step makes an important contribution to k_{cat} in this mutant. APH(3′)-IIIa Met26Pro also does not display a significant solvent isotope

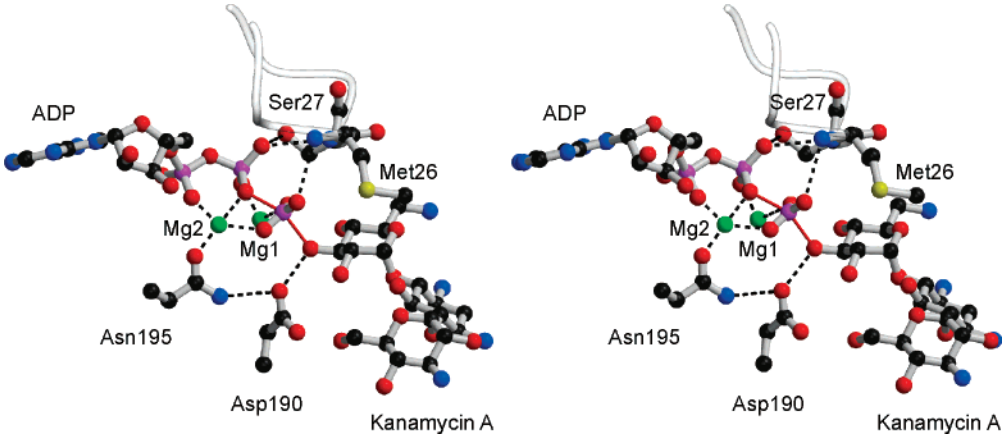

FIGURE 4: Stereoview of the transition state model of the phosphoryl transfer reaction catalyzed by APH(3′)-IIIa.

Table 3: MIC Determinations with Kanamycin A for *E. coli* BL21(DE3) Expressing APH(3′)-IIIa Wild-Type and Mutant Proteins

construct	MIC (μg/mL) for kanamycin A
BL21(DE3)/pET22b control	2
WT	1024
Ser27Ala	64
Ser27Pro	4
Met26Ala	512
Met26Pro	128

effect (Table 2), paralleling the wild-type and Ser27Ala results.

The magnesium dependence of Met26Ala is similar to WT where activity decreases with increasing metal ion concentration, whereas Met26Pro shows a pattern similar to the Ser27 mutations (Figure 3). The change in the magnesium dependence patterns in the Ser27 and Met26Pro mutants, alongside the lack of a solvent viscosity effect for these mutants, strongly suggests a change to the factors governing the turnover rate. The results for the Met26 mutants are unlikely to be due to misfolded enzyme, as protease sensitivity patterns for these mutants were identical to wild-type patterns (data not shown).

In Vivo Effects of NPL Mutants. For a comparison to the in vitro kinetic data, MICs for *Escherichia coli* carrying the WT and mutated resistance determinants were compared to the MICs for *E. coli* without an aminoglycoside resistance determinant. Consistent with the in vitro effects, mutation of Met26 to Ala appeared to have little effect, whereas there were significant decreases in MICs for the Ser27 and Met26Pro mutants (Table 3). Mutation of Ser27 to Pro had the largest effect, where the MIC was nearly indistinguishable from *E. coli* without an aminoglycoside resistance determinant.

DISCUSSION

The enzyme APH(3′)-IIIa from Gram-positive pathogenic bacteria is the most thoroughly studied aminoglycoside resistance kinase and as such represents the paradigm for this class of antibiotic resistance enzyme. We have recently shown through site-directed mutagenesis, metal ion dependence, solvent isotope, and solvent viscosity experiments that the phosphate transfer mechanism employed by this enzyme is most consistent with a dissociative-like mechanism of phosphoryl transfer with generation of a metaphosphate-like transition state (*3*). These results are consistent with a growing body of evidence that suggests several kinases adopt dissociative-like phosphoryl transfer mechanisms, e.g., the Tyr protein kinase, Csk (*15*, *16*), which is structurally homologous to APH(3′)-IIIa, and other kinases such as hexokinase (*17*). The degree to which phosphoryl transfer by APH(3′)-IIIa adopts a dissociative character, however, is not known, and a continuum of possibilities, from completely dissociative to fully associative, is possible in this class of enzyme (*18*).

The recently determined crystal structures of APH(3′)-IIIa in the absence of ligands and bound with the ATP analogue AMPPNP (*8*), and bound with kanamycin and ADP (*9*), have complemented the existing structural information available for the ADP-bound enzyme (*1*). These structures reveal that the NPL undergoes a significant rearrangement (7 Å at its tip; residue 25) upon nucleotide binding, and we postulate that this loop, like analogous regions in protein kinases, could play a mechanistic role in aminoglycoside phosphorylation. In particular, the contributions of Ser27, which is ubiquitously present in all APH(3′) enzymes, and Met26, a residue that molecular modeling indicated could be important in loop movement and nucleotide binding during catalysis, were analyzed by a variety of methods.

Results of steady-state kinetic experiments on the Ser27Ala mutant, in combination with the lack of a viscosity effect for this mutant and the change in magnesium dependence pattern, revealed that the hydroxyl group of this residue is important for phosphoryl transfer. Kinetic characterization of the Ser27Pro mutant further demonstrated the importance of this residue to catalysis, as the effect on k_{cat} of a Ser to Pro change is 10-fold greater than the effect of a Ser to Ala change. These results suggest that, in addition to the Ser27 functional group, the backbone amide is also important for rate enhancement.

Although Ser27 is clearly important to rate enhancement, its role was not immediately obvious from available ground state structures. On the basis of the evidence gathered thus far, suggesting that phosphoryl transfer proceeds through a dissociative like mechanism, and keeping in mind the dynamics of the NPL, especially considering the addition of a hydrogen bond to the β-phosphate by the Ser27 backbone amide in the presence of aminoglycoside, we constructed a model of the predicted transition state structure

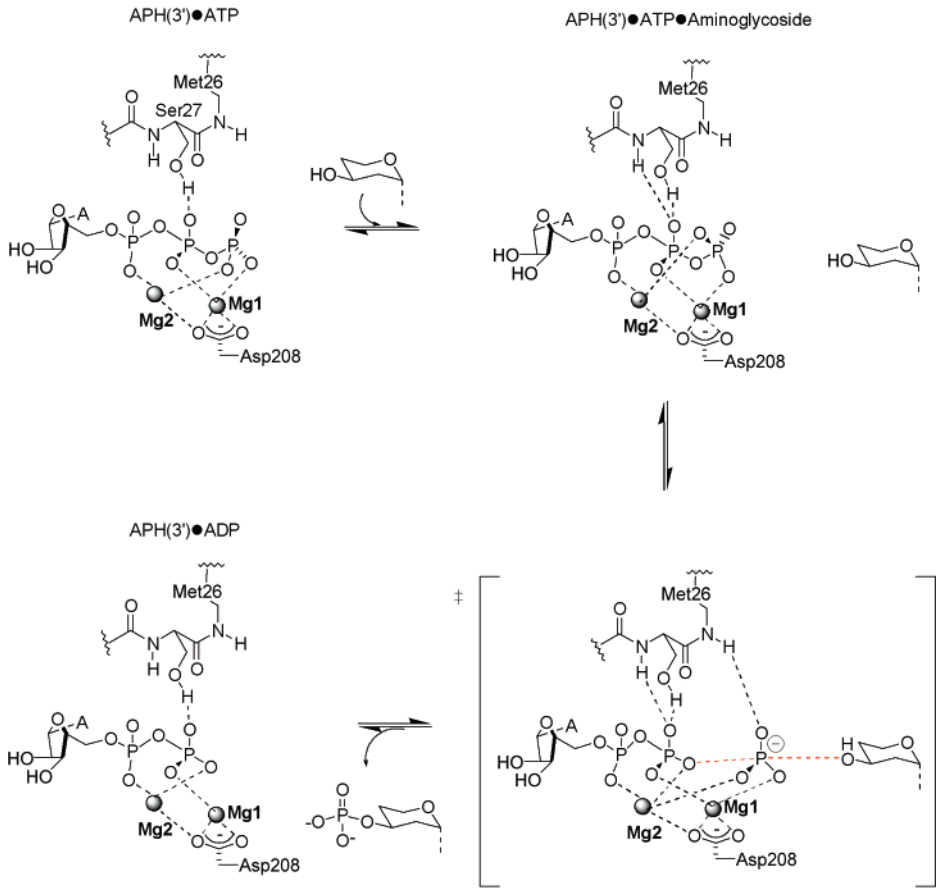

FIGURE 5: Proposed role of the nucleotide positioning loop in APH(3′)-IIIa-catalyzed phosphoryl transfer. Formal changes on phosphates are not shown for clarity.

in the APH(3′)-IIIa active site. These modeling studies suggested the formation of a hydrogen bond between the backbone amide of Met26 to the γ-phosphate during phosphoryl transfer that is not obvious in any ground state structures of APH(3′)-IIIa solved thus far. This hypothesis was then investigated by generating appropriate Met26 mutants. Met26Ala was not significantly impaired in its ability to phosphorylate aminoglycosides where k_{cat}, comparable to the WT enzyme, was still largely governed by a viscosity-dependent rate, likely ADP release. In contrast, phosphoryl transfer catalyzed by the Met26Pro mutant was significantly decreased compared to the WT enzyme, where the chemical step has likely become rate-limiting on the basis of the lack of a solvent viscosity effect and the change in the magnesium dependence pattern. Thus, although the side chain of Met26 does not appear to be important to catalysis, consistent with the lack of conservation of this residue, the backbone amide likely plays a role in phosphoryl transfer as suggested by our modeling studies. It must be acknowledged that steady-state kinetic comparisons of WT APH(3′)-IIIa to mutant proteins likely underrepresents the quantitative contribution of residues involved in catalysis, as the rate-determining step in the WT enzyme is not group transfer but ADP release (*12*). A similar case arises in protein kinase A, where pre-steady-state analysis has suggested that the phosphoryl transfer step is 25 times faster than ADP release (*19*). Thus, for example, although steady-state kinetic comparisons of the Met26Pro mutant to WT suggest a decrease in k_{cat} of 10-fold, the actual chemical step may be decreased much more substantially, which would be consistent with the loss of a hydrogen-bonding interaction from the backbone amide, a function that parallels the role of Ser53 in protein kinase A, where a similar decrease in catalytic activity occurred with the Ser53Pro mutant (*7*).

Both Met26 and Ser27 clearly play roles in enhancing the rate of aminoglycoside phosphorylation by APH(3′)-IIIa where these roles are primarily catalytic as the majority of the effect is seen as a decrease in k_{cat} when these residues are mutated. Ser27, especially as it forms an additional hydrogen bond to a nonbridging oxygen of the nucleotide β-phosphate group from its side chain to its backbone amide, may play an important role in situating Met26 for its interaction with the transferred phosphate. However, considering that the mutation of Ser27Pro is more deleterious than the mutation of Met26Pro, Ser27 may play additional role(s) to enhance catalysis.

The results obtained are consistent with a model of phosphoryl transfer where NPL residues Ser27 and Met26 play important roles (Figure 5). Upon Mg-ATP binding, the NPL region undergoes a conformation change permitting the formation of a hydrogen bond between the hydroxymethyl group of Ser27 forms and a β-phosphate nonbridge oxygen; the other nonbridge oxygen on the β-phosphate acts as a ligand to Mg1. Mg1 also interacts with the γ-phosphate of ATP and is linked to the enzyme via the invariant and essential Asp208; thus this magnesium ion is positioned as a fulcrum from which phosphoryl transfer occurs. In a dissociative mechanism, the γ-PO bond must lengthen to generate the elongated transition state, and it follows that the interaction between Mg1 and the β-phosphate must be

weakened so that the γ-phosphate is able to be transferred. Upon binding aminoglycoside, APH(3′)-IIIa undergoes a conformational change in the NPL such that the side chain of Ser27 begins to translate away and the amide backbone of Ser27 is pressed toward the β-phosphate. These events help to turn the β-phosphate on its axis, and as the nonbridge oxygens of the γ- and β-phosphates begin to eclipse, the repulsion between the two phosphates will increase and the γ-PO bond will weaken. The structure of APH(3′)-IIIa in complex with ADP and kanamycin A reveals an additional hydrogen bond to the β-phosphate nonbridge oxygen by the Ser27 backbone amide. Therefore, during group transfer, this addition must occur along with bond breakage between the β- and γ-phosphate, resulting in a net increase in distance between Mg1 and its β-phosphate oxygen ligand. The importance of the amide of Met26 would therefore lie in stabilization of the metaphosphate, possibly through a direct interaction (Figure 5). The NPL therefore serves as a lever working with Mg1 to facilitate the requisite $\beta-\gamma$ phosphate bond breakage necessary for generation of the metaphosphate-like TS.

CONCLUSIONS

Our previous results have suggested that APH(3′)-IIIa catalyzes phosphoryl transfer through a dissociative mechanism with an expanded transition state. We have demonstrated through structural modeling, site-directed mutagenesis, and kinetic and in vivo analysis that the nucleotide positioning loop plays an important part in the phosphoryl transfer reaction. It should be possible to use this information to develop compounds that mimic the metaphosphate-like transition state and take advantage of the unique interactions that are not available in the ground state, such as the hydrogen bond from the backbone amide of Met26. A potent inhibitor of insulin receptor kinase has previously been designed on the basis of an assumed dissociative mechanism (*20*), and likewise, potent inhibitors of APH(3′)-IIIa can be designed with appropriate characteristics that should be able to reverse aminoglycoside resistance in vivo.

REFERENCES

1. Hon, W. C., McKay, G. A., Thompson, P. R., Sweet, R. M., Yang, D. S. C., Wright, G. D., and Berghuis, A. M. (1997) *Cell 89*, 887−895.
2. Daigle, D. M., McKay, G. A., Thompson, P. R., and Wright, G. D. (1999) *Chem. Biol. 6*, 11−18.
3. Boehr, D. D., Thompson, P. R., and Wright, G. D. (2001) *J. Biol. Chem. 276*, 23929−23936.
4. Hemmer, W., McGlone, M., Tsigelny, I., and Taylor, S. S. (1997) *J. Biol. Chem. 272*, 16946−16954.
5. Grant, B. D., Hemmer, W., Tsigelny, I., Adams, J. A., and Taylor, S. S. (1998) *Biochemistry 37*, 7708−7715.
6. Hirai, T. J., Tsigelny, I., and Adams, J. A. (2000) *Biochemistry 39*, 13276−13284.
7. Aimes, R. T., Hemmer, W., and Taylor, S. S. (2000) *Biochemistry 39*, 8325−8332.
8. Burk, D. L., Hon, W. C., Leung, A. K., and Berghuis, A. M. (2001) *Biochemistry 40*, 8756−8764.
9. Fong, D. H., and Berghuis, A. M. (2002) *EMBO J.* (in press).
10. McKay, G. A., Thompson, P. R., and Wright, G. D. (1994) *Biochemistry 33*, 6936−6944.
11. Leatherbarrow, R. J. (2000) Erithacus Software Ltd., Staines, U.K.
12. McKay, G. A., and Wright, G. D. (1996) *Biochemistry 35*, 8680−8685.
13. Northrop, D. B. (1998) *J. Chem. Educ. 75*, 1153−1157.
14. McKay, G. A., and Wright, G. D. (1995) *J. Biol. Chem. 270*, 24686−24692.
15. Kim, K., and Cole, P. A. (1997) *J. Am. Chem. Soc. 119*, 11096−11097.
16. Kim, K., and Cole, P. A. (1998) *J. Am. Chem. Soc. 120*, 6851−6858.
17. Jones, J. P., Weiss, P. M., and Cleland, W. W. (1991) *Biochemistry 30*, 3634−3639.
18. Mildvan, A. S. (1997) *Proteins 29*, 401−416.
19. Grant, B. D., and Adams, J. A. (1996) *Biochemistry 35*, 2022−2029.
20. Parang, K., Till, J. H., Ablooglu, A. J., Kohanski, R. A., Hubbard, S. R., and Cole, P. A. (2001) *Nat. Struct. Biol. 8*, 37−41.

BI0256680